Available online at www.sciencedirect.com
ScienceDirect
IFAC PapersOnLine 58-29 (2024) 118–123

Modeling and Parameter Optimization of Battery Liquid Cooling Thermal Management System for Electric Vehicles ⋆

Baolin Ma * **Lulu Guo** ** [1] **Hong Chen** **

* *Shanghai Research Institute for Intelligent Autonomous Systems, Tongji University, Shanghai 200092, PR China*
** *Department of Control Science and Engineering, Tongji University, Shanghai 201804, PR China*

Abstract: In this paper, a control-oriented electrothermal coupling battery liquid cooling thermal management model is presented, which includes the refrigeration cycle of the air-conditioning system, the cooling cycle of the battery system, and the battery electric-thermal coupled loop in electric vehicles. A cool-down mode is considered for the battery thermal management system in the hot summer. A high-fidelity physical-based model is established in Simcenter AMESim to validate the effectiveness of the proposed control-oriented model. The simulation results show that the deviations of the vehicle speed, battery state of charge, and temperature between the AMESim and proposed model are within 0.84km/h, 0.13%, and 0.23°C, respectively. Besides, the validation results show the same trend of the proposed dynamic character as AMESim, which indicates the proposed model is well suited for controller design in the future.

Keywords: battery thermal management system, liquid cooling modeling, two-phase flow heat transfer, electric vehicles.

1. INTRODUCTION

With the rapid development of intelligence, interconnection, and electrification trends, clean energy and technology play a key role in smart cities (Razmjoo et al. (2022)). Especially, electric vehicles (EVs) as the representatives of clean energy vehicles, are gradually replacing traditional vehicles and hybrid EVs (Xing et al. (2021)), and the process of the connected and autonomous vehicles further promotes the development of EVs (Kopelias et al. (2020)). However, due to the fewer universal charging stations and lower charging rates compared with gas stations, range anxiety, as a primary factor, directly affects consumer acceptance when choosing EVs as daily transportation tools. In the extreme temperature environment (e.g. hot summer or cold winter), the overall vehicle energy consumption mainly supplies the thermal demand of the cabin and battery pack, in addition to traction energy consumption. Meanwhile, the energy consumption cost by cabin thermal demand can account for up to 30% in summer, and 35% in winter (Erjavec (2012)), sometimes the proportions would be higher. As for cabin and battery heating conditions, positive temperature coefficient (PTC), as the most effective way, is still used for winter heating, so it hardly solves the energy-saving problem (Zhou et al. (2022)). Besides, heat pump technology is used for improving the heating efficiency in mild environment conditions (ambient temperature higher than -10°C) by a 4-way valve for reversing the refrigerant flow changing between cooling and heating operation. In addition, the waste heat recovery of the driving motors is also a heat resource in the thermal sustaining stage (Tian et al. (2020)). For cabin cooling thermal management, several model-based model predictive control (MPC) strategies are utilized to improve the efficiency of the heating, ventilation, and air conditioning (HVAC) system with the sensitivity related to vehicle real speed (Guo et al. (2024); Ma et al. (2023)).

For battery cooling thermal management in hot summer, there are three main cooling styles, i.e. air-cooling, liquid-cooling, and other hybrid cooling strategies Mali et al. (2021). The air-cooling strategy has a simple structure and low Operation and maintenance costs. The cooling air can be divided into three types, i.e. outside environment air, cabin air from the HVAC, and cooling air from the evaporator base vapor compression cycle. For example, a control strategy integrated with different single flow types based on the temperature difference among battery cells is proposed for a designed parallel air cooling battery thermal management system (BTMS) (Chen et al. (2024)), and the numerical results show the proposed strategy can reduce the temperature difference effectively. However, the cooling performance is low compared with liquid cooling, especially in the case of high-power applications to maintain the temperature in an optimal operation zone, such as rapid acceleration and deceleration conditions. Besides, too much noise generated by the high rotation speed of the fan and blower is also a disadvantage that restricts the development of an air-cooling strategy in BTMS of

⋆ This work was supported in part by the National Natural Science Foundation of China under Grant 62203334, Shanghai Rising-Star Program under Grant 22YF1451300, and in part by the Fundamental Research Funds for the Central Universities.
[1] Corresponding author (e-mail: guoll21@tongji.edu.cn).

10.1016/j.ifacol.2024.11.130

EVs. For the liquid-cooling strategy, there are two loops to achieve the heat generated from the battery moving to ambient for the secondary liquid-cooling structure. One is the radiator with an electric fan structure, the other is that the coolant takes away the heat load from the battery pack, while the coolant heat load is carried away the refrigerant by the vapor and compression cycle of the air-conditioning system. The cooling loop selection depends on the ambient temperature and the cooling load. When the ambient temperature is lower than the liquid coolant temperature, the liquid coolant flows to the radiator by the outside air cooling. However, when the exterior temperature is higher than the liquid coolant temperature, liquid flow through the chiller exchanges heat load with the refrigerant so that the battery can be easily cooled by an effective AC cooling cycle. A stochastic MPC is applied to BTMS with a second cooling system with the probability of battery heat generation using historical driving data in a stochastic sense, and the energy-saving is improved significantly within maintaining an acceptable temperature regulation performance, compared to other control strategies (Park and Ahn (2020)). The hybrid cooling styles are mainly combined multi-cooling styles, such as air-cooling and liquid-cooling (Hu et al. (2023)), air-cooling based on phase change material (Jilte et al. (2019)), and so on.

For BTMS modeling, several works simplify the two-phase flow heat transfer of the heat exchangers, i.e. condenser and evaporator/chiller. Amini et al. (2020); Hu et al. (2023) proposed a 2-order dynamic model of battery state of charge and temperature with the direct air-cooling and liquid-cooling capacities as the control input. However, this method can not be applied in the actual BTMS execution system. To solve the indirect control problem of BTMS, Park and Ahn (2020) proposed a 2-order dynamic model of battery and coolant temperatures, and the vapor and compression cycle of the refrigerant is assumed to be fixed, ignoring the impact of changes in rotation speed of compressor and pump. Chen et al. (2022) proposed a 4-order control-oriented HVAC and battery cooling dynamic model according to a high-fidelity physics-based model developed in MATLAB/Simulink, but the electrothermal coupling character of the battery pack is ignored.

To address the above issue, this paper presents a 6-order electrothermal coupling BTMS dynamic model, with 3 direct actuator control variables: electric-driven motor torque, compressor speed, and coolant pump speed. Besides, the proposed control-oriented model is validated with a high-fidelity BTMS model in Simcenter AMESim environment.

The structure of this article is organized as follows. Section 2 presents the battery pack and cooling system model. Section 3 presents the parameter optimization of the proposed model and the validation of the model through an open-loop simulation. Finally, the conclusion and future work are given in Section 4.

2. BATTERY PACK AND COOLING SYSTEM MODEL

The vehicle under investigation is an electric passenger vehicle with the liquid cooling BTMS, shown as Fig. 1, and the vehicle powertrain system driven by a single-motor. This section establishes the battery thermal and powertrain dynamic models, including battery thermal, AC/liquid cooling, and vehicle longitudinal dynamic models.

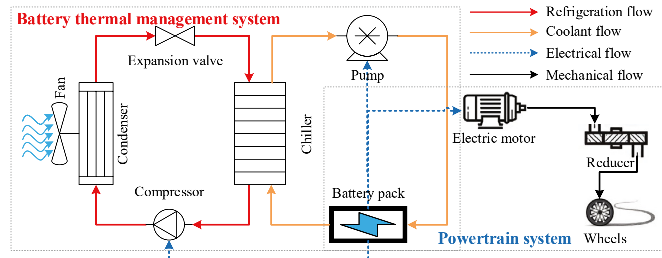

Fig. 1. The structure of single-motor driven EVs with BTMS.

2.1 Electric-thermal Coupled Model of Battery Pack

The battery pack current I_{bat} can be derived from the equivalent circuit model as:

$$I_{\mathrm{bat}} = \frac{V_{\mathrm{oc}} - \sqrt{V_{\mathrm{oc}}^2 - 4P_{\mathrm{bat}}R_{\mathrm{int}}}}{2R_{\mathrm{int}}} \tag{1}$$

where the open-circuit voltage V_{oc} and the internal resistance R_{int} are functions of the battery pack state of charge (SoC) SOC and temperature T_{bat}, i.e., $V_{\mathrm{oc}} = f(SOC, T_{\mathrm{bat}}), R_{\mathrm{int}} = f(SOC, T_{\mathrm{bat}})$. The output power of battery pack P_{bat} satisfies:

$$P_{\mathrm{bat}} = P_{\mathrm{trac}} + P_{\mathrm{btms}} \tag{2}$$

where P_{trac} and P_{btms} are the traction power and BTMS power (mainly includes power consumption of compressor and coolant pump) of the battery pack, and can be expressed as follows:

$$P_{\mathrm{trac}} = N_{\mathrm{m}} M_{\mathrm{m}} (\eta_{\mathrm{m}} \eta_{\mathrm{b}})^{-\mathrm{sign}(M_{\mathrm{m}})} \tag{3a}$$

$$P_{\mathrm{btms}} = P_{\mathrm{comp}} + P_{\mathrm{pump}} \tag{3b}$$

where N_{m}, M_{m}, and η_{m} are the rotation speed, torque, and efficiency of the electric motor, η_{b} is the battery efficiency, respectively. P_{comp} and P_{pump} are the power of the compressor and pump, which would be given in the subsection 2.4. To facilitate optimization problem solving, the EM system power model is given as:

$$P_{\mathrm{trac}} = \sum_{i=0}^{2} \sum_{j=0}^{2} p_{\mathrm{m},ij} N_{\mathrm{m}}^{i} M_{\mathrm{m}}^{j} \tag{4}$$

where the parameters $p_{\mathrm{m},ij}$ can be obtained by curve fitting using the least square method. Additionally, the EM required torque can obtained by the longitudinal dynamic model:

$$\begin{aligned} \dot{v}_{\mathrm{veh}} =& \frac{M_{\mathrm{m}} I_{\mathrm{r}}}{r_{\mathrm{w}} m_{\mathrm{veh}}} \eta_{\mathrm{r}}^{\mathrm{sgn}(M_{\mathrm{m}})} - \mathrm{g}\sin(\theta) - \mu \mathrm{g}\cos(\theta) \\ & - \frac{\rho_{\mathrm{air}} A_{\mathrm{f}} C_{\mathrm{d}} v_{\mathrm{veh}}^2}{2m_{\mathrm{veh}}} \end{aligned} \tag{5}$$

$$N_{\mathrm{m}} = \frac{30 v_{\mathrm{veh}} I_{\mathrm{r}}}{\pi r_{\mathrm{w}}} \tag{6}$$

The battery pack SoC as a main indicator to evaluate energy, can be given as follows:

$$\dot{SOC} = -\frac{I_{\mathrm{bat}}}{C_{\mathrm{bat}}} = -\frac{V_{\mathrm{oc}} - \sqrt{V_{\mathrm{oc}}^2 - 4P_{\mathrm{bat}}R_{\mathrm{int}}}}{2C_{\mathrm{bat}}R_{\mathrm{int}}} \tag{7}$$

where C_{bat} is the battery capacity.

Meanwhile, during the working process (charging or discharging) of the battery pack, the temperature is another main indicator that influences the battery pack's performance, such as safety and output characters. According to the laws of thermodynamics, the thermal dynamic model of a battery pack can be expressed as follows:

$$m_{\mathrm{bat}} c_{\mathrm{bat}} \dot{T}_{\mathrm{bat}} = \dot{Q}_{\mathrm{gen}} - \dot{Q}_{\mathrm{air}} - \dot{Q}_{\mathrm{dis}} \tag{8}$$

where m_{bat} and c_{bat} are the lumped mass and thermal capacity of the battery pack, and $\dot{Q}_{\mathrm{gen}}$, $\dot{Q}_{\mathrm{air}}$ and $\dot{Q}_{\mathrm{dis}}$ are the heat load of the battery pack generation, natural convection heat transfer and liquid cooling dissipation. The heat generated $\dot{Q}_{\mathrm{gen}}$ includes two parts: joule heating and entropy change, as

$$\dot{Q}_{\mathrm{gen}} = I_{\mathrm{bat}}^2 R_{\mathrm{int}} - I_{\mathrm{bat}} T_{\mathrm{bat}} \frac{\mathrm{d}V_{\mathrm{oc}}}{\mathrm{d}T_{\mathrm{bat}}} \tag{9}$$

where T_{bat} is battery pack temperature, and $\frac{\mathrm{d}V_{\mathrm{oc}}}{\mathrm{d}T_{\mathrm{bat}}}$ is the entropic coefficient.

$\dot{Q}_{\mathrm{air}}$ is mainly composed of convective heat exchange $Q_{\mathrm{air,conv}}$ and radiative heat exchange $Q_{\mathrm{air,rad}}$, which can be expressed as:

$$\dot{Q}_{\mathrm{air,conv}} = h_{\mathrm{bat2amb}} A_{\mathrm{bat2amb}} (T_{\mathrm{bat}} - T_{\mathrm{amb}}) \tag{10a}$$

$$\dot{Q}_{\mathrm{air,rad}} = \varepsilon_{\mathrm{bat}} \sigma A_{\mathrm{bat2amb}} (T_{\mathrm{bat}}^4 - T_{\mathrm{amb}}^4) \tag{10b}$$

where h_{bat2amb} and A_{bat2amb} are convective heat exchange coefficient and area between battery pack and ambient environment, T_{amb} is the ambient temperature, $\varepsilon_{\mathrm{bat}}$ is the equivalent emission factor of the battery pack surface, and σ is the Stefan-Boltzmann constant.

2.2 Refrigeration Loop Model of AC system

In this study, the heat exchange stages of the condenser and chiller are assumed at a quasi-steady state (i.e. neglecting the thermodynamic dynamics). Therefore, the refrigerant side heat exchange $\dot{Q}_{\mathrm{cond,r}}$ and air side heat exchange $\dot{Q}_{\mathrm{cond,air}}$ of the condenser can be computed as follows:

$$\dot{Q}_{\mathrm{cond,r}} = \dot{m}_{\mathrm{r}} (h_{\mathrm{comp,out}} - h_{\mathrm{cond,out}}) \tag{11a}$$

$$\dot{Q}_{\mathrm{cond,air}} = \epsilon_{\mathrm{air}} \dot{m}_{\mathrm{air}} c_{\mathrm{air}} (T_{\mathrm{r,comp,out}} - T_{\mathrm{amb}}) \tag{11b}$$

where $h_{\mathrm{comp,out}}$ and $h_{\mathrm{cond,out}}$ are the specific enthalpy of the refrigerant flow at the compressor outlet and condenser outlet, $\dot{m}_{\mathrm{r}}$ is the refrigerant flow mass rate of the compressor. $\dot{m}_{\mathrm{air}}$, c_{air} and T_{amb} are the air flow mass rate, thermal capacity and temperature of the external environment, ϵ_{air} is the air correction factor related to $\dot{m}_{\mathrm{air}}$, and $T_{\mathrm{r,comp,out}}$ is the refrigerant temperature of the compressor outlet, which can be computed based on the refrigerant temperature of the condenser outlet $T_{\mathrm{cond,out}}$ and $h_{\mathrm{comp,out}}$. Under the adiabatic expansion valve assumption, the specific enthalpy of the refrigerant flow at the chiller inlet $h_{\mathrm{chil,in}}$ equals to $h_{\mathrm{cond,out}}$, i.e. $h_{\mathrm{chil,in}} = h_{\mathrm{cond,out}}$. Hence, the refrigerant side heat exchange $\dot{Q}_{\mathrm{chil,r}}$ and coolant side heat exchange $\dot{Q}_{\mathrm{chil,c}}$ of the chiller can be expressed as follows:

$$\dot{Q}_{\mathrm{chil,r}} = \dot{m}_{\mathrm{r}} (h_{\mathrm{cond,out}} - h_{\mathrm{chil,out}}) \tag{12a}$$

$$\dot{Q}_{\mathrm{chil,c}} = \epsilon_{\mathrm{c}} \dot{m}_{\mathrm{c}} c_{\mathrm{c}} (T_{\mathrm{c,bat,out}} - T_{\mathrm{r,chil,out}}) \tag{12b}$$

where $\dot{m}_{\mathrm{c}}$ and c_{c} are the flow mass rate and thermal capacity of the coolant, ϵ_{c} is the coolant correction factor related to $\dot{m}_{\mathrm{c}}$, $T_{\mathrm{c,bat,out}}$ and $T_{\mathrm{r,chil,out}}$ are the temperature of the coolant at the battery outlet and the refrigerant at chiller outlet, $h_{\mathrm{chil,out}}$ is the specific enthalpy of the refrigerant flow at the chiller outlet.

$\dot{m}_{\mathrm{air}}$ is related to the real vehicle speed v_{veh} as:

$$\dot{m}_{\mathrm{air}} = \rho_{\mathrm{air}} A_{\mathrm{cond}} v_{\mathrm{veh}} + \dot{m}_{\mathrm{air,park}} \tag{13}$$

where A_{cond} is the convective area between the condenser and external environment and $\dot{m}_{\mathrm{air,park}}$ is the equivalent air flow rate when the vehicle is parking. $\dot{m}_{\mathrm{c}}$ depends on the rotation speed of the pump ω_{pump} as:

$$\dot{m}_{\mathrm{c}} = f(\omega_{\mathrm{pump}}) \tag{14}$$

Assuming the refrigeration cycle is an ideal vapor-compression cycle, the refrigerant at the condenser outlet and the chiller outlet are saturated liquid and saturated vapor, respectively. Therefore, the specific enthalpy of the refrigerant flow at the condenser outlet $h_{\mathrm{cond,out}}$ and chiller outlet $h_{\mathrm{chil,out}}$ can be given as:

$$h_{\mathrm{cond,out}} = a_1 T_{\mathrm{r,cond,out}} + b_1 \tag{15a}$$

$$h_{\mathrm{chil,out}} = a_2 T_{\mathrm{r,chil,out}} + b_2 \tag{15b}$$

where $a_{1,2}$ and $b_{1,2}$ are the temperature correlation coefficients, which can be obtained by the REFPROP software (Lemmon et al. (2002)). In this study, the R134a refrigerant is selected, and the parameters are: $a_1 = 1.603, b_1 = 192.2, a_2 = 0.5384, b_2 = 398.6$. It should be noted that the above simplifications in this subsection aim to reduce the model's complexity while retaining its effectiveness for control design.

The specific enthalpy of the refrigerant flow at the compressor outlet $h_{\mathrm{comp,out}}$ is a function of $h_{\mathrm{chil,out}}$ and the specific enthalpy increasing of the compressor Δh_{comp} as:

$$h_{\mathrm{comp,out}} = h_{\mathrm{chil,out}} + \Delta h_{\mathrm{comp}} \tag{16}$$

where Δh_{comp} can be expressed as the function of $T_{\mathrm{r,cond,out}}$, $T_{\mathrm{r,chil,out}}$ and the refrigerant flow mass rate $\dot{m}_{\mathrm{r}}$ (Chen et al. (2022)) as:

$$\Delta h_{\mathrm{comp}} = f(T_{\mathrm{r,cond,out}} - T_{\mathrm{r,chil,out}}, \dot{m}_{\mathrm{r}}) \tag{17}$$

where $\dot{m}_{\mathrm{r}}$ can be calculated as follows:

$$\dot{m}_{\mathrm{r}} = \eta_{\mathrm{comp,vol}} \omega_{\mathrm{comp}} \rho_{\mathrm{r}} V_{\mathrm{comp}} \tag{18}$$

where $\eta_{\mathrm{comp,vol}}$, ω_{comp} and V_{comp} are volumetric efficiency, rotary speed, and displacement of the compressor, respectively. ρ_{r} is refrigerant density.

2.3 Cooling Loop of Battery Pack

$\dot{Q}_{\mathrm{dis}}$ can be formulated by a uniform wall temperature model as:

$$\dot{Q}_{\mathrm{dis}} = U_{\mathrm{bat2c}} A_{\mathrm{bat}} (T_{\mathrm{bat}} - T_{\mathrm{c,bat,out}}) \tag{19}$$

where A_{bat} is the convective area between the battery pack and coolant and the heat exchange coefficient U_{bat2c} is computed as follows:

$$U_{\mathrm{bat2c}} = k_{\mathrm{bat2c}} \frac{Nu_{\mathrm{c}} \lambda_{\mathrm{c}}}{l_{\mathrm{pipe}}} \tag{20}$$

where k_{bat2c} is the gain on heat exchange, λ_{c} is the thermal conductivity of coolant, and l_{pipe} is characteristic length of the cooling pipe. The turbulent Nusselt value Nu_{c} can be computed as:

$$j_{\mathrm{fact}} = 0.665 Re_{\mathrm{c}}^{-0.5} \tag{21a}$$

$$Nu_{\mathrm{c}} = j_{\mathrm{fact}} Re_{\mathrm{c}} Pr_{\mathrm{c}}^{1/3} = 0.665 Re_{\mathrm{c}}^{0.5} Pr_{\mathrm{c}}^{1/3} \tag{21b}$$

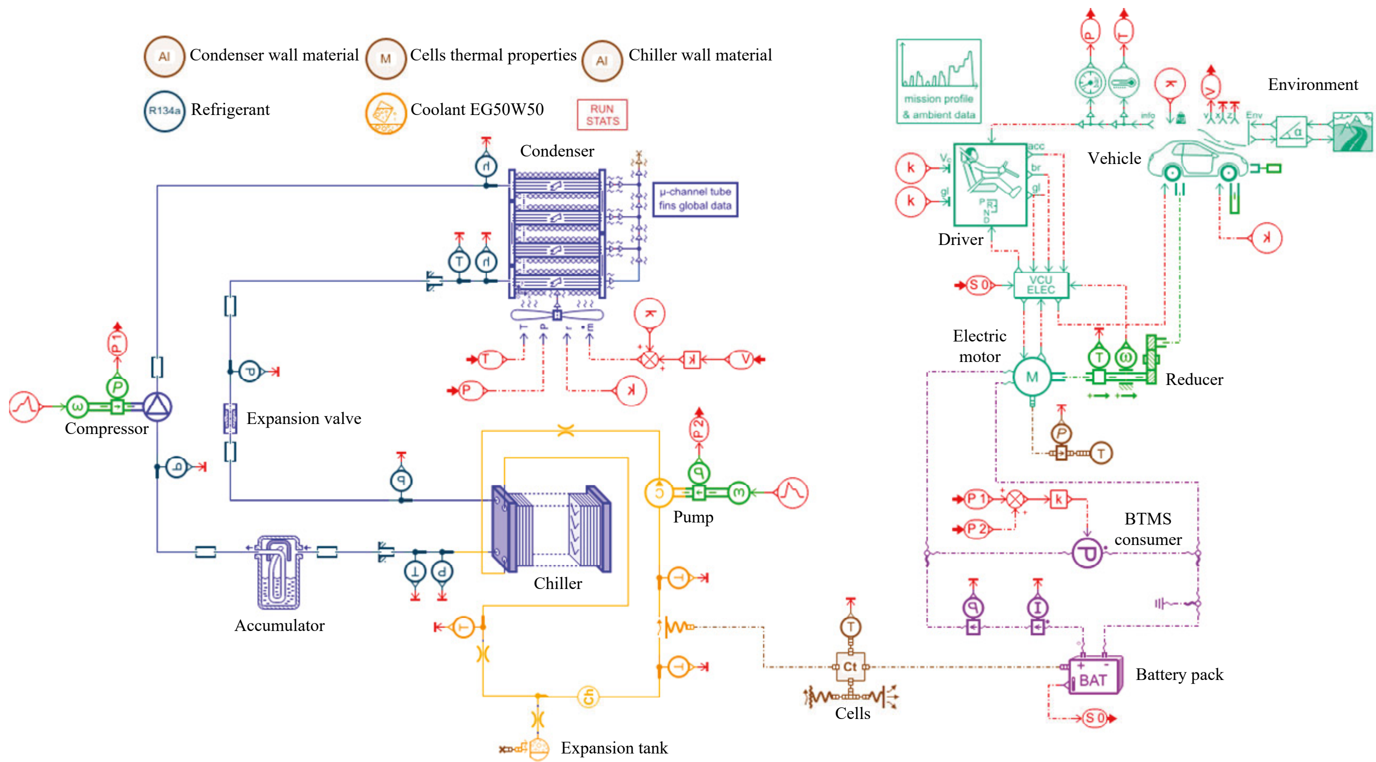

Fig. 2. AMESim model of EVs battery pack liquid cooling thermal management system.

where j_{fact} is the Colburn j-factor. The Reynolds number Re_{clnt} and Plante number Pr_{c} can be calculated with:

$$Re_{\text{c}} = \frac{\rho_{\text{c}} v_{\text{c}} l_{\text{pipe}}}{\mu_{\text{c}}} \tag{22a}$$

$$Pr_{\text{c}} = \frac{\mu_{\text{c}} c_{\text{c}}}{\lambda_{\text{c}}} \tag{22b}$$

where ρ_{c}, v_{c}, λ_{c}, and c_{c} are the density, flow velocity, thermal capacity and specific heat capacity of the coolant. μ_{c} is the absolute viscosity of the coolant inside the pipe at coolant temperature and l_{pipe} is the characteristic length of the cooling pipe.

According to eqs. (20-22), the heat exchange coefficient U_{bat2c} can be obtained as follows:

$$U_{\text{bat2c}} = 0.665 k_{\text{bat2c}} \frac{\rho_{\text{c}}^{0.5} c_{\text{c}}^{1/3} \lambda_{\text{c}}^{2/3}}{\mu_{\text{c}}^{1/6} l_{\text{pipe}}^{0.5}} v_{\text{c}}^{0.5}$$

The coolant temperature of the chiller outlet $T_{\text{c,chil,out}}$ can be obtained with a steady-state equation as follows:

$$T_{\text{c,chil,out}} = T_{\text{c,bat,out}} + \frac{\dot{Q}_{\text{chil,c}}}{\dot{m}_{\text{c}} c_{\text{c}}} \tag{23}$$

2.4 Power Consumption Model of Battery Pack Thermal Management System

Typically, the power consumption of BTMS mainly comprises the energy costs from the compressor and coolant pump (denoted as P_{comp} and P_{pump}), i.e. $P_{\text{btms}} = P_{\text{comp}} + P_{\text{pump}}$. Meanwhile, the electric power consumption of the compressor P_{comp} can be expressed as:

$$P_{\text{comp}} = \frac{\dot{m}_{\text{rfg}} \Delta h_{\text{comp}}}{\eta_{\text{comp,mech}}} \tag{24}$$

where $\eta_{\text{comp,mech}}$ is the mechanical efficiency of the compressor.

As for the power consumption of the pump P_{pump}, it can be calculated as:

$$P_{\text{pump}} = \frac{V_{\text{clnt}} \Delta p_{\text{pump}}}{\eta_{\text{pump}}}$$

where Δp_{pump} is the pressure difference between the outlet and inlet of the pump, which can be represented as the function of the pump rotation speed and coolant flow rate $\Delta p_{\text{pump}} = f(V_{\text{clnt}})$, and η_{pump} is the global efficiency of the pump. Due to the proportional relationship between V_{clnt} and ω_{pump}, P_{pump} can be rewritten as a polynomial relationship finally:

$$P_{\text{pump}} = f(\omega_{\text{pump}}) = \sum_{i=0}^{3} p_i \omega_{\text{pump}}^i \tag{25}$$

where fitting parameters p_i are: $p_0 = -6.001\text{e}-1$, $p_1 = 3.031\text{e}-3$, $p_2 = -4.114\text{e}-6$ and $p_3 = 7.849\text{e}-9$, in which the model accuracy R-square is 1.0000 and RMSE is 0.6813 W.

2.5 Summary of the Battery Pack and Cooling System Dynamic Mode

According to the description of the above subsections (2.1-2.3), the discretization based on first order low pass filter and forward Euler method of EVs battery pack liquid cooling thermal management dynamic model can be summary as follows, which have six state variables $\boldsymbol{x} = [v_{\text{veh}}, SOC, T_{\text{cond}}, T_{\text{chil}}, T_{\text{c}}, T_{\text{bat}}]^T$ and three control variables $\boldsymbol{u} = [M_{\text{m}}, \omega_{\text{comp}}, \omega_{\text{pump}}]^T$. To simplify the variable nomenclature, some variables define: $T_{\text{cond}} := T_{\text{r,cond,out}}$, $T_{\text{chil}} = T_{\text{r,chil,out}}$ and $T_{\text{c}} = T_{\text{c,bat,out}}$.

$$
\begin{aligned}
v_{\mathrm{veh},k+1} =& v_{\mathrm{veh},k} + \dot{v}_{\mathrm{veh},k}\Delta t \\
=& f(x_{1,k}, u_{1,k}) \qquad (26a) \\
SOC_{k+1} =& SOC_k + S\dot{O}C_k \Delta t \\
=& f(x_{1,k}, x_{2,k}, x_{3,k}, x_{4,k}, u_{1,k}, u_{2,k}, u_{3,k}) \qquad (26b) \\
T_{\mathrm{cond},k+1} =& T_{\mathrm{cond},k} + \frac{-\dot{Q}_{\mathrm{cond,air},k} + \dot{Q}_{\mathrm{cond,r},k}}{a_1 \dot{m}_{\mathrm{r},k}\tau_{\mathrm{r}}}\Delta t \\
=& f(x_{1,k}, x_{3,k}, x_{4,k}, u_{2,k}) \qquad (26c) \\
T_{\mathrm{chil},k+1} =& T_{\mathrm{chil},k} + \frac{\dot{Q}_{\mathrm{chil,r},k} + \dot{Q}_{\mathrm{chil,c},k}}{(a_2 \dot{m}_{\mathrm{r},k} + \epsilon_{\mathrm{c},k}\dot{m}_{\mathrm{c},k}c_{\mathrm{clnt}})\tau_{\mathrm{r}}}\Delta t \\
=& f(x_{3,k}, x_{4,k}, x_{5,k}, u_{2,k}, u_{3,k}) \qquad (26d) \\
T_{\mathrm{c},k+1} =& T_{\mathrm{c},k+1} + \frac{\dot{m}_{\mathrm{c},k}c_{\mathrm{c}}(T_{\mathrm{c,chil,out},k} - T_{\mathrm{c},k}) + \dot{Q}_{\mathrm{dis},k}}{(\dot{m}_{\mathrm{c},k}c_{\mathrm{c}} + U_{\mathrm{bat2c}}A_{bat})\tau_{\mathrm{c}}}\Delta t \\
=& f(x_{4,k}, x_{5,k}, x_{6,k}, u_{3,k}) \qquad (26e) \\
T_{\mathrm{bat},k+1} =& T_{\mathrm{bat},k} + \dot{T}_{\mathrm{bat},k}\Delta t \\
=& f(x_{1,k}, x_{2,k}, x_{5,k}, x_{6,k}, u_{1,k}, u_{3,k}) \qquad (26f)
\end{aligned}
$$

where Δt is the dynamic system sample time. The time constants of first order low pass filterτ_{r} and τ_{c} are identified as the most significant parameters that directly influence the BTMS temperature response characters. Additionally, they would be tuned in the subsection 3.1.

3. PARAMETER OPTIMIZATION AND MODEL VALIDATION

3.1 Parameter optimization

For unknown parameters stated in subsection 2.5, there are 2 parameters, i.e. $\tau_{r,c}$ that need to be tuned. The cost function is to minimize the sum of thermal system temperature weighted deviations, considering the BTMS model is mainly used to calibrate battery temperature. Therefore, the optimization problem of parameters to be tuned can be expressed as:

$$
\begin{aligned}
&\tau_{\mathrm{r}}^*, \tau_{\mathrm{c}}^* = \arg_{\tau_{\mathrm{r}},\tau_{\mathrm{c}}} \min \sum_{k=t_0}^{t_{\mathrm{f}}} J_k \\
&\text{s.t.} \quad J_k = ((T_{\mathrm{cond},k} - \hat{T}_{\mathrm{cond},k})^2 + (T_{\mathrm{chil},k} - \hat{T}_{\mathrm{chil},k})^2) \\
&\qquad + \alpha_1 (T_{\mathrm{c},k} - \hat{T}_{\mathrm{c},k})^2 + \alpha_2 (T_{\mathrm{bat},k} - \hat{T}_{\mathrm{bat},k})^2 \\
&\qquad \hat{v}_{\mathrm{veh},k+1} = f_{vveh}(\hat{v}_{\mathrm{veh},k}) \\
&\qquad S\hat{O}C_{k+1} = f_{soc}(S\hat{O}C_k) \\
&\qquad \hat{T}_{\mathrm{cond},k+1} = f_{Tcond}(\hat{T}_{\mathrm{cond},k}) \qquad (27) \\
&\qquad \hat{T}_{\mathrm{chil},k+1} = f_{Tchil}(\hat{T}_{\mathrm{chil},k}) \\
&\qquad \hat{T}_{\mathrm{c},k+1} = f_{Tc}(\hat{T}_{\mathrm{c},k}) \\
&\qquad \hat{T}_{\mathrm{bat},k+1} = f_{Tbat}(\hat{T}_{\mathrm{bat},k}) \\
&\qquad \hat{v}_{\mathrm{veh},0} = v_{\mathrm{veh},0}, S\hat{O}C_0 = SOC_0 \\
&\qquad \hat{T}_{\mathrm{cond},0} = T_{\mathrm{cond},0}, \hat{T}_{\mathrm{chil},0} = T_{\mathrm{chil},0} \\
&\qquad \hat{T}_{\mathrm{c},0} = T_{\mathrm{c},0}, \hat{T}_{\mathrm{bat},0} = T_{\mathrm{bat},0}
\end{aligned}
$$

where t_0 and t_{f} are the initial and terminal instants, x and $\hat{x}$ denote the variable of real and control-oriented model variable, f_{vveh}, f_{soc}, f_{Tcond}, f_{Tchil}, f_{Tc} and f_{Tbat} are the functions corresponding to eqs.(26a-26f), $\alpha_{1,2}$ are the weight parameters. The optimization problem can be solved by numerical iteration methods such as sequence quadratic programming (SQP), which is a powerful optimization method to solve constrained nonlinear optimization problems. The SQP method balances efficiency and accuracy by solving a sequence of quadratic programming subproblems. At the same time, quadratic approximations often capture the local behavior of nonlinear problems effectively, thus enabling SQP to converge to an optimal solution with superlinear convergence rates. Moreover, by incorporating both equality and inequality constraints directly into the subproblems, SQP provides a systematic way to handle complex constrained problems while maintaining robustness and flexibility in diverse applications. These two aspect advantages are provided by the SQP method, compared to other optimization algorithms, such as genetic algorithms or simulated annealing.

Table 1. Main parameters and corresponding values.

Parameter	Value [Unit]	Parameter	Value [Unit]
ρ_{air}	1.205 [kg/m^3]	A_{f}	2.2 [m^2]
C_{d}	0.306 [-]	m_{veh}	1600 [kg]
μ	0.01 [-]	r_{w}	0.32 [m]
I_{r}	10 [-]	η_{r}	0.98 [-]
c_{bat}	795 [J/kg/K]	C_{bat}	98 [Ah]
T_{amb}	35 [°C]	c_{air}	1016.65 [J/kg/K]
ρ_{c}	1.069e3 [kg/m^3]	μ_{c}	4.563e-3 [kg/m/s]
c_{c}	3.310e3 [J/kg/K]	λ_{c}	4.156e-1 [W/m/K]

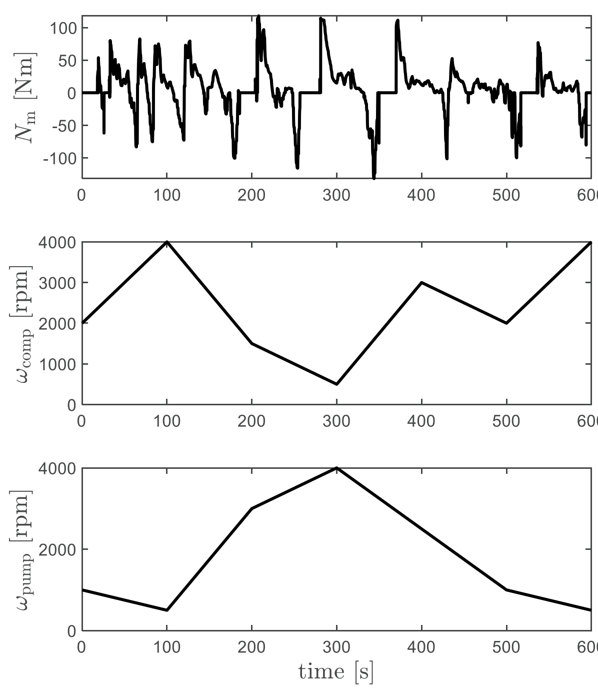

Fig. 3. Control variables of Liquid cooling thermal management system, (a) electric motor torque, (b) compressor speed, (c) pump speed.

3.2 Control-oriented Model Validation

To validate the efficiency of the control-oriented model, a high-fidelity physics-based battery pack liquid cooling thermal management system of EVs has been developed in simcenter AMESim shown as Fig. 2. The Main parameters of the vehicle system and integrated battery pack thermal management system are shown in Table 1.

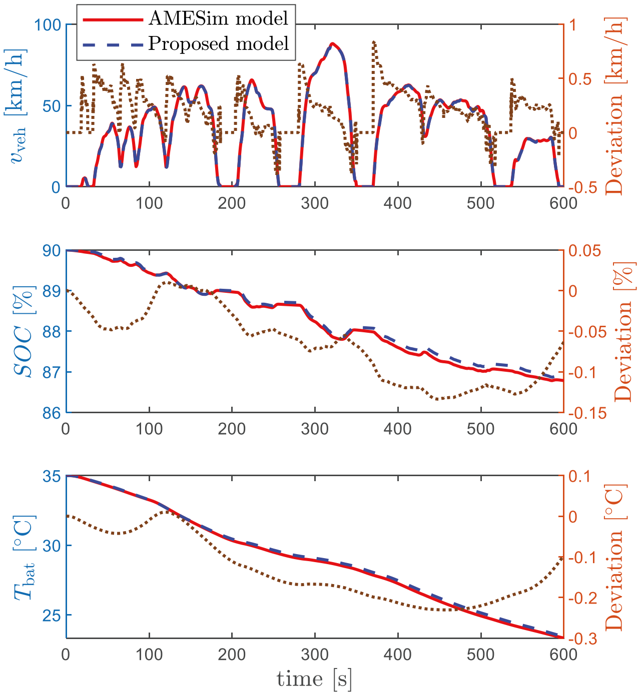

Fig. 4. Comparison of state variables of Liquid cooling thermal management system between the AMESim and proposed model, (a) vehicle speed, (b) battery SOC, (c) battery temperature.

The driving cycle is under SC03, the electric motor output torque is computed based on the driver model in AMESim shown in Fig. 3(a), and the other control variables, compressor and pump speeds, are given as shown in Fig. 3(b,c). The states comparison between AMESim simulation and open-loop simulation of the proposed control-oriented model are shown in Fig. 4, the model deviations of vehicle speed, battery SoC, and battery temperature are within 0.84km/h, 0.13%, and 0.23°C. Therefore, the experiment results show that the proposed control-oriented model with high accuracy can be used for model-based controller design in the future.

4. CONCLUSION AND FUTURE WORK

In this paper, a high-fidelity physical-based battery liquid cooling thermal management system is developed in AMESim platform. The proposed control-oriented model using simplified models for two-phase heat exchangers is established to reduce complexity. Compared to the AMESim model, the simulation of battery SoC and temperature is accurate on a system level, but much more explicit and simplified.

In the future, the proposed control-oriented model will be utilized to develop optimal control strategies based on MPC algorithm, which might enable better decision-making of BTMS controller adopting a more suitable strategy to enhance operational efficiency, reduce energy consumption, and improve the all-electric range of EVs.

REFERENCES

Amini, M.R., Kolmanovsky, I., and Sun, J. (2020). Hierarchical mpc for robust eco-cooling of connected and automated vehicles and its application to electric vehicle battery thermal management. *IEEE Transactions on Control Systems Technology*, 29(1), 316–328.

Chen, K., Zhang, Z., Wu, B., Song, M., and Wu, X. (2024). An air-cooled system with a control strategy for efficient battery thermal management. *Applied Thermal Engineering*, 236, 121578.

Chen, Y., Kwak, K.H., Kim, J., Jung, D.D., and Kim, Y. (2022). Control-oriented model of hvac and battery cooling systems in electric vehicles. *IFAC-PapersOnLine*, 55(37), 44–49.

Erjavec, J. (2012). *Hybrid, electric, and fuel-cell vehicles*. Cengage Learning.

Guo, L., Ma, B., Gong, X., Hu, Y., and Chen, H. (2024). Bilevel predictive control for hevs integrating energy and cabin thermal comfort. *IEEE Transactions on Transportation Electrification*, 10(1), 623–634.

Hu, Y., Deng, N., Gong, X., Sun, Y., and Chen, H. (2023). Energy consumption optimisation of a battery thermal management system for electric vehicles considering different cooling modes. *International journal of vehicle design*, 92(2-4), 128–148.

Jilte, R.D., Kumar, R., Ahmadi, M.H., and Chen, L. (2019). Battery thermal management system employing phase change material with cell-to-cell air cooling. *Applied Thermal Engineering*, 161, 114199.

Kopelias, P., Demiridi, E., Vogiatzis, K., Skabardonis, A., and Zafiropoulou, V. (2020). Connected & autonomous vehicles–environmental impacts–a review. *Science of the total environment*, 712, 135237.

Lemmon, E.W., Huber, M.L., and McLinden, M.O. (2002). Nist reference fluid thermodynamic and transport properties–refprop. *NIST standard reference database*, 23(2002), v7.

Ma, B., Chu, F., Guo, L., Hu, Y., Xu, F., and Chen, H. (2023). Real-time predictive control for evs cabin thermal management considering air quality. *IEEE Transactions on Transportation Electrification*, 1–1.

Mali, V., Saxena, R., Kumar, K., Kalam, A., and Tripathi, B. (2021). Review on battery thermal management systems for energy-efficient electric vehicles. *Renewable and Sustainable Energy Reviews*, 151, 111611.

Park, S. and Ahn, C. (2020). Computationally efficient stochastic model predictive controller for battery thermal management of electric vehicle. *IEEE Transactions on Vehicular Technology*, 69(8), 8407–8419.

Razmjoo, A., Gandomi, A.H., Pazhoohesh, M., Mirjalili, S., and Rezaei, M. (2022). The key role of clean energy and technology in smart cities development. *Energy Strategy Reviews*, 44, 100943.

Tian, Z., Gu, B., Gao, W., and Zhang, Y. (2020). Performance evaluation of an electric vehicle thermal management system with waste heat recovery. *Applied Thermal Engineering*, 169, 114976.

Xing, J., Leard, B., and Li, S. (2021). What does an electric vehicle replace? *Journal of Environmental Economics and Management*, 107, 102432.

Zhou, X., Chen, H., Liang, K., Wang, W., Dong, B., and Zhang, Y. (2022). Winter performance analysis of multi-mode integrated thermal management system based on thermodynamics. *Sustainable Energy Technologies and Assessments*, 53, 102726.